Far-infrared spectroscopy of modulated and ferroelectric betaine calcium chloride dihydrate

1993 J. Phys.: Condens. Matter 5 4401

(http://iopscience.iop.org/0953-8984/5/26/012)

J. Phys.: Condens. Matter 5 (1993) 4401–4418. Printed in the UK

Far-infrared spectroscopy of modulated and ferroelectric betaine calcium chloride dihydrate

S Kamba†, V Dvořák†, J Petzelt†, Yu G Goncharov‡, A A Volkov‡ and G V Kozlov‡

† Institute of Physics, Czechoslovak Academy of Sciences, Na Slovance 2, 18040 Prague 8, Czech Republic

‡ Institute of General Physics, Russian Academy of Sciences, Vavilov Street 38, 117942 Moscow, Russia

Received 8 January 1993

Abstract. Far-infrared and near-millimetre transmission and reflectivity measurements of betaine calcium chloride dihydrate were carried out between 300 and 15 K. All modes below 300 cm^{-1} were classified according to symmetry and their wavevectors q using selection rules for mode activation in the modulated phases. Almost all activated modes with $q \neq 0$ can be assigned assuming condensation of the single order parameter of Λ_3 symmetry ($P_y(k)$ wave). In the low-temperature homogeneous ferroelectric phase, traces of modulated phases are observed depending on the sample clamping. On the basis of our assignment the dispersion curves of the eight lowest phonon branches along the modulation direction were constructed for the four main modulated phases (incommensurate and commensurate with $\delta = \frac{1}{4}, \frac{1}{3}, \frac{1}{6}$). The behaviour of amplitudons and pseudophasons is discussed. The previously observed $E \| y$ mode below 10 cm^{-1} in the incommensurate phase has been assigned to the inhomogeneous $\Lambda_2(c^* - 2k)$ mode (c^* is the reciprocal-lattice vector and k the modulation wavevector).

1. Introduction

Betaine calcium chloride dihydrate (BCCD) $(CH_3)_3NCH_2COO{\cdot}CaCl_2 \cdot 2H_2O$ has been intensively investigated recently owing to its unique very rich sequence of phase transitions (PTs) (Brill and Ehses 1985, Unruh *et al* 1989). Upon lowering the temperature, at $T_1 = 164$ K, it undergoes the first PT from the space group $Pnma$ ($Z = 4$) (Rother *et al* 1984) to an incommensurate (IC) phase with modulation along the c direction (Brill *et al* 1985) (modulation wavevector $k_i = \delta(T)c^*$, where $\delta(T_1) \simeq 0.32$). On cooling, $\delta(T)$ decreases and passes through many (at least 15) commensurate (C) values and four IC phases in between, realizing in this way an incomplete devil's staircase (Unruh *et al* 1989). Finally, at $T_{16} = 46$ K it locks into a uniform ($\delta(T_{16}) = 0$) ferroelectric phase. In table 1 we list all the main phases with their suggested δ-values and observed components of the spontaneous polarization P_s. Under hydrostatic pressure (Ao *et al* 1989) or bias electric field (Freitag and Unruh 1990) the variety of C and IC phases still increases by structure-branching processes.

Pérez-Mato (1988) described the whole PT sequence using a superspace group approach with a single order parameter $P_y(k)$ of Λ_3 symmetry. However, Kroupa *et al* (1990) observed a slight rotation of the optical indicatrix below T_1 (about 2°) which suggested that the situation might be more complicated. The simplest explanation of an indicatrix rotation consists in adopting a small monoclinic distortion below T_1, i.e. assuming a change in the point group $mmm \rightarrow 2/m$. It is well known that, with a single order parameter,

0953-8984/93/264401+18$07.50

Table 1. Phase transitions in BCCD (after Unruh *et al* 1989). The phases 2, 4, 6 and 8 are in fact composed of IC and very narrow C phases.

Phase	Transition temperature (K)	$\delta(c^*)$	P_s (observed components)
1		0	—
	$T_1 = 164.0$	0.32	
2		$\simeq$0.30	—
	$T_2 = 127.8$		
3		$\frac{2}{7}$	P_y
	$T_3 = 124.5$		
4		$\simeq$0.28	—
	$T_4 = 118.4$		
5		$\frac{3}{11}$	—
	$T_5 = 117.4$		
6		$\simeq$0.27	—
	$T_6 = 116.0$		
7		$\frac{4}{15}$	P_y
	$T_7 = 115.7$		
8		$\simeq$0.26	—
	$T_8 = 115.3$		
9		$\frac{1}{4}$	P_x
	$T_9 = 75.8$		
10		$\frac{2}{9}$	P_y
	$T_{10} = 75.2$		
11		$\frac{1}{5}$	—
	$T_{11} = 53.3$		
12		$\frac{2}{11}$	P_y
	$T_{12} = 53.0$		
13		$\frac{1}{6}$	P_x
	$T_{13} = 47.1$		
14		$\frac{2}{13}$	P_y
	$T_{14} = 46.9$		
15		$\frac{1}{7}$	—
	$T_{15} = 46.2$		
16		$\frac{1}{8}$	P_x
	$T_{16} = 46.0$		
17		0	P_y

no point group symmetry change can be achieved in the IC phase (Dvořák *et al* 1983). Therefore Dvořák *et al* (1988) and Dvořák (1990) suggested that lowering of the point group from mmm to $2/m$ might be due to condensation of two order parameters with the same wavevector k triggered by biquadratic coupling between them. The symmetry of these order parameters should be Λ_3 ($P_y(k)$ parameter) and Λ_2 ($Q(k)$ parameter). It should be pointed out that rotation of the indicatrix has been observed in IC phases of other materials too, namely in $(TMA)_2CuCl_4$ (Uesu and Kobayashi 1985) and $BaMnF_4$ (Kobayashi and Kleemann 1990). So far this effect is not fully understood but is very probably connected with the finite wavelength of light propagating in a inhomogeneously modulated medium (Dvořák 1991) and not necessarily with a homogeneous monoclinic deformation of the lattice. It was also suggested that a small anomaly Δn_{yz} in the birefringence about 0.3 K below T_1 (Kroupa *et al* 1990) might indicate the second triggered PT where the second order parameter freezes in. However, the existence of this transition was recently disproved in a

thorough dielectric measurement by Wilhelm and Unruh (1991). Also the recent thorough x-ray structural analyses at 130 K (Zúñiga *et al* 1991) and 90 K (Ezpeleta *et al* 1992) give no indication of the second order parameter. Therefore for BCCD finally the interesting idea of the simultaneous freezing of two IC waves has been abandoned (Dvořák 1991).

Very recently (Almeida *et al* 1992) performed a thorough neutron diffraction experiment on partially deuterated BCCD. To explain the anomalous temperature decrease in the intensity of diffraction satellites near 80 K (in the $\delta = \frac{1}{5}$ phase 11) they suggested a triggered freezing of the second order parameter $Q(k)$ at this temperature. This could then also explain the presence of a small $P_s \| x$ component below 47 K in the ferroelectric phase 17 (Ribeiro *et al* 1990).

In this paper we shall deal with detailed far-infrared (FIR) and millimetre-wavelength data on BCCD, their evaluation, analysis of selection rules and mode assignment. It will be shown that nearly all features can be explained by assuming one frozen order parameter but that two order parameters cannot be excluded at low temperatures. Brief preliminary data of this work have already been published (Kamba *et al* 1990) and also our earlier data on the $\epsilon_y^*(\nu)$ complex dielectric function are available (Volkov *et al* 1986, Goncharov *et al* 1988).

2. Experimental details

BCCD single crystals were grown from aqueous solution by evaporation at temperatures of 310–315 K (Rother *et al* 1984). Plane-parallel samples of (001), (010) and (101) orientation and about 10 mm diameter were cut and polished. Owing to various transparencies for different spectral regions and polarizations the sample thickness was varied between 0.3 and 3 mm.

Two different IR measurement techniques were used. A home-built quasi-optic Epsilon spectrometer based on backward-wave-oscillator (BWO) sources (Volkov *et al* 1985) and a Fourier transform interferometer Bruker IFS 113v were used in the 8–23 cm^{-1} and 13–650 cm^{-1} ranges, respectively. In the former technique the polarized power transmittance and phase shift of the transmitted wave were measured simultaneously to calculate directly the complex permittivity spectra $\epsilon^*(\nu) = \epsilon'(\nu) - i\epsilon''(\nu)$ in the case of the less transparent polarization $E \| y$. In the case of the highly transparent $E \| x$ and $E \| z$ polarizations, only the power transmittance was measured, but a pronounced interference pattern enabled us to determine the complete dielectric response as well.

In the case of the Fourier transform spectrometer we used both normal power reflection and transmission measurements. Reflectivity spectra can be correctly measured only in regions of sample opacity (13–650 cm^{-1} for $E \| y$, and 50–650 cm^{-1} for $E \| x, z$). Transmission spectra were taken from 13 to 90 cm^{-1} for $E \| x, z$ while the polarization $E \| y$ has been measured by Ao and Schaack (1988a). For the region below 100 cm^{-1} a liquid-helium-cooled Ge bolometer was used. For the measurements in a cryostat (15–300 K), special care was taken to prevent mechanical clamping of the sample.

3. Results and evaluation

In figure 1 we present the reflectivity spectra for all three polarizations $E \| x, y, z$. The spectra were analysed using the Kramers–Kronig relations in a standard way to calculate finally the complex dielectric response. The resulting $\epsilon''(\nu)$ spectra are shown in figure 2.

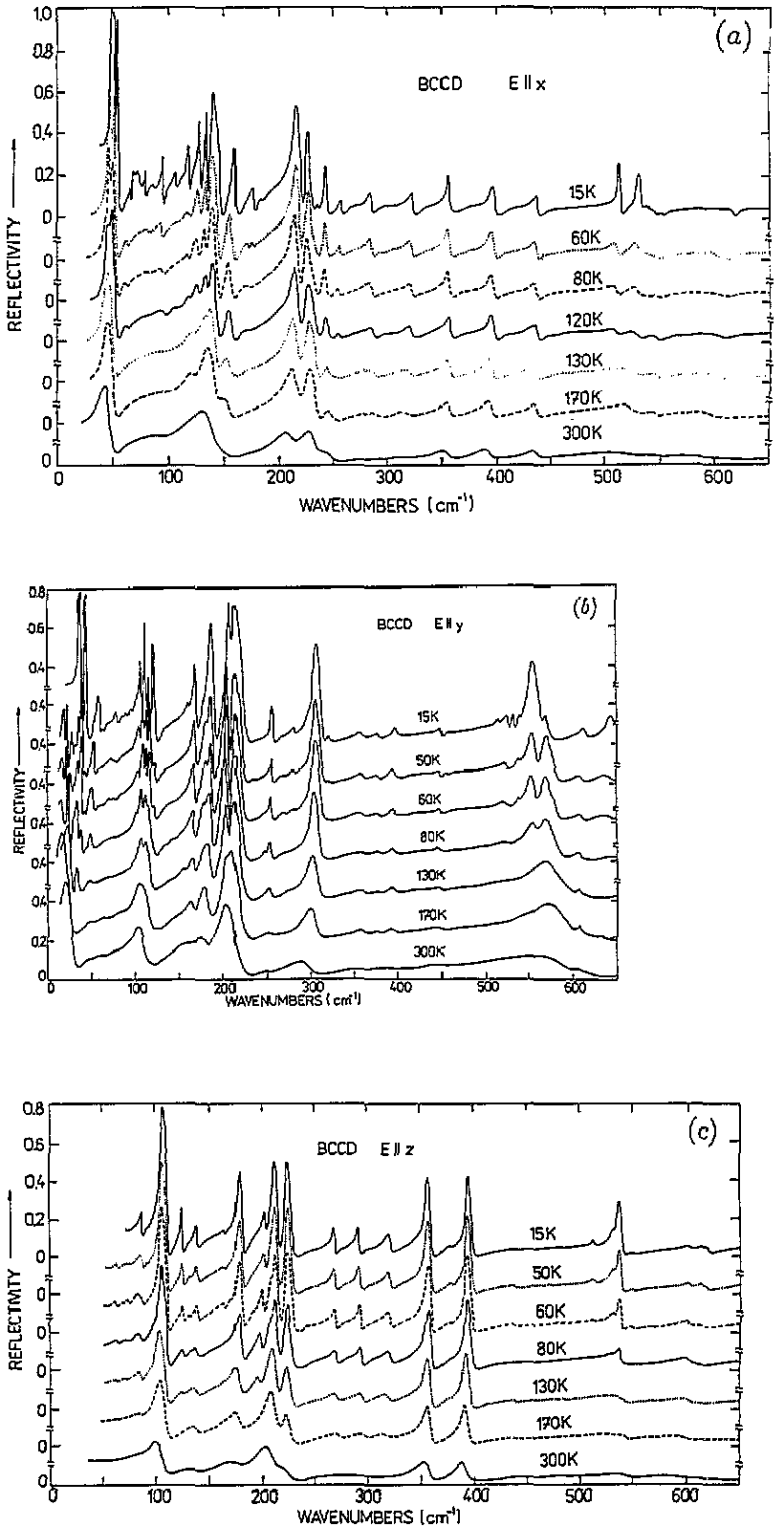

Figure 1. FIR reflectivity spectra of BCCD at different temperatures for (*a*) $E \| x$, (*b*) $E \| y$ and (*c*) $E \| z$ polarizations.

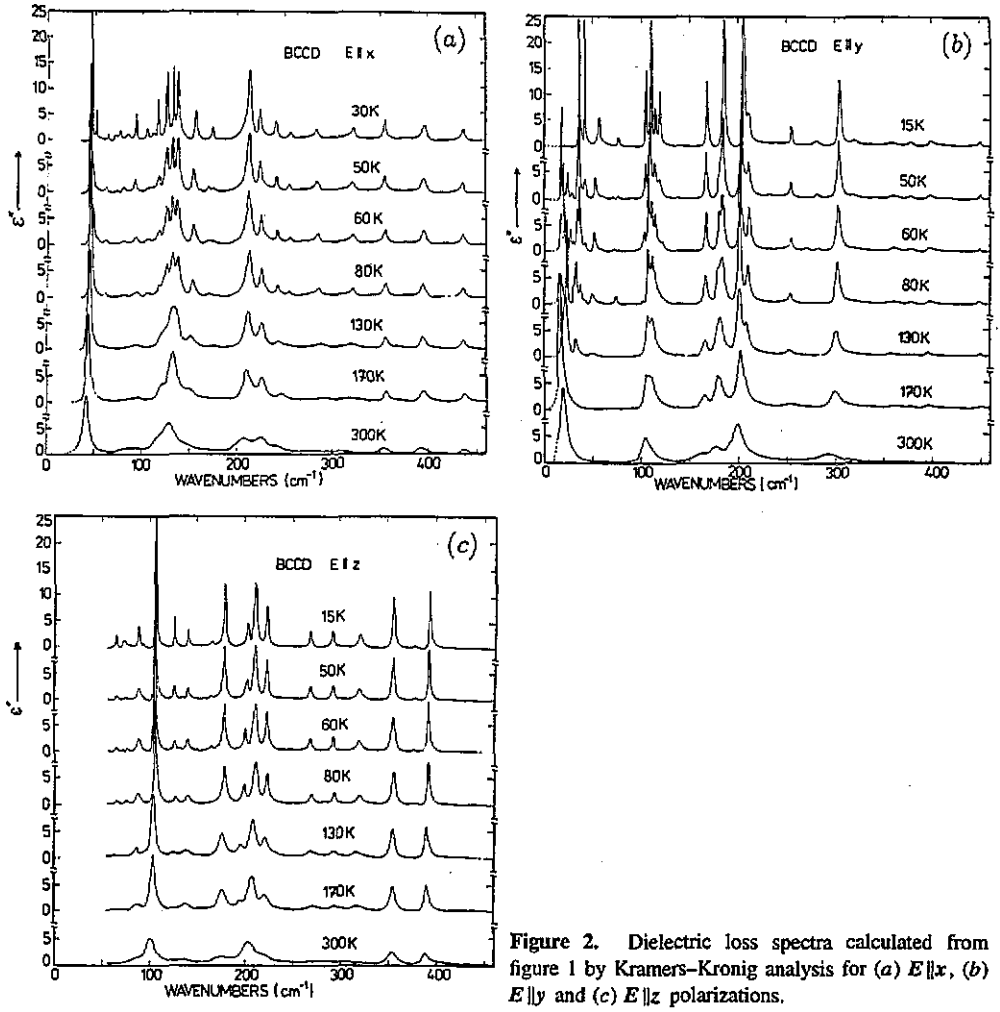

Figure 2. Dielectric loss spectra calculated from figure 1 by Kramers–Kronig analysis for (*a*) $E \| x$, (*b*) $E \| y$ and (*c*) $E \| z$ polarizations.

Each peak in the $\epsilon''(\nu)$ spectra represents a transverse polar optic phonon mode. Note the pronounced increase in active mode numbers in the modulated phases.

In figure 3 the transmission spectra are shown for the $E \| x$ and $E \| z$ polarizations in the 13–90 cm^{-1} range. In figure 4 the $E \| x, z$ transmission spectra on thicker samples are shown in the 17–24 cm^{-1} range. The modes can be clearly distinguished from the regular interference pattern and their frequencies were evaluated from the corresponding transmission minima. From the interferences at the low-frequency end we calculated that $\epsilon_x'(10\ cm^{-1}, 40\ K) = 5.7$, $\epsilon_z'(10\ cm^{-1}, 290\ K) = 3.9$ and $\epsilon_z'(10\ cm^{-1}, 50\ K) = 3.7$.

In figure 5 we show the complex dielectric spectra $\epsilon_y^*(\nu)$ at 44 and 11 K evaluated from our new measurements on stress-free samples. Only one weak mode (at 22.3 cm^{-1}) is seen in contrast with the seven modes seen in our earlier experiment (Volkov *et al* 1986, Goncharov *et al* 1988) where no special care was taken to prevent mechanical clamping of the sample. This agrees with the difference between the early structural data (Brill and Ehses 1985), suggesting that $\delta = \frac{1}{6}$ for the lowest-temperature phase and the general opinion nowadays (Unruh *et al* 1989, Ao and Schaack 1988a, b) which indicates a non-modulated structure ($\delta = 0$) for this phase in the stress-free sample.

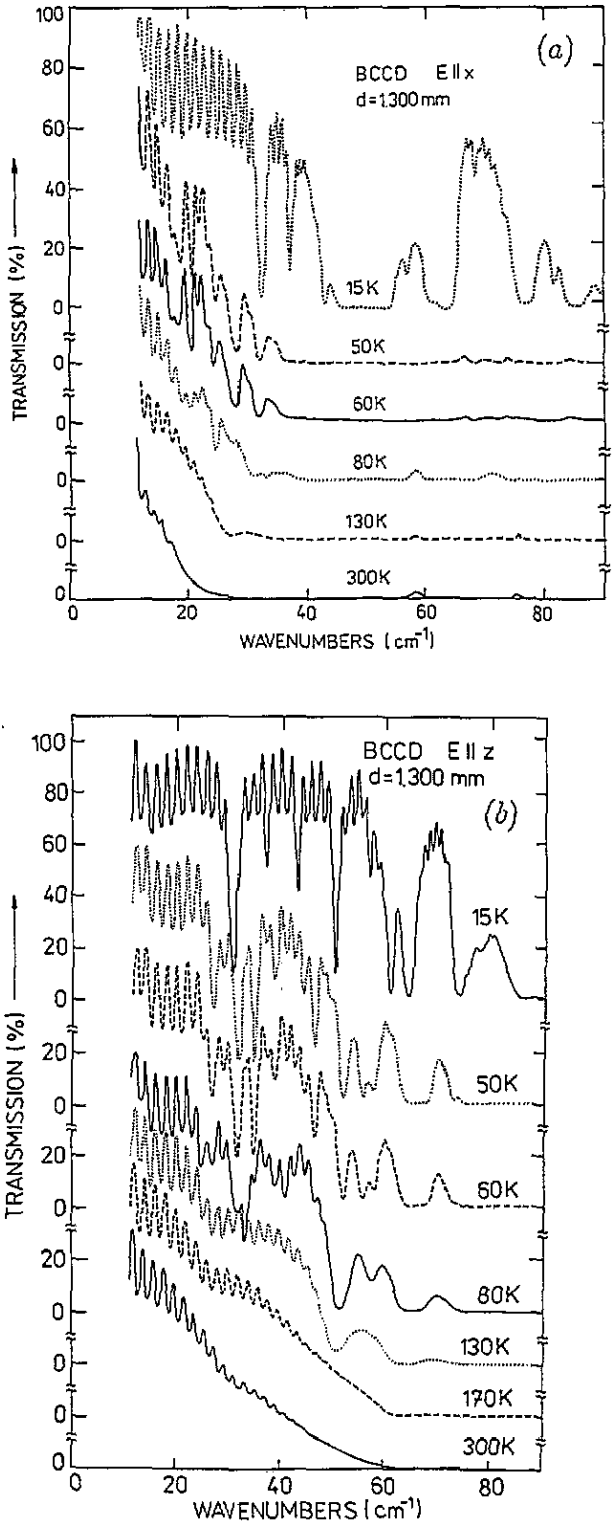

Figure 3. Temperature dependences of the FIR transmission spectra for (*a*) $E \| x$ and (*b*) $E \| z$ polarizations (sample thickness $d = 1.3$ mm).

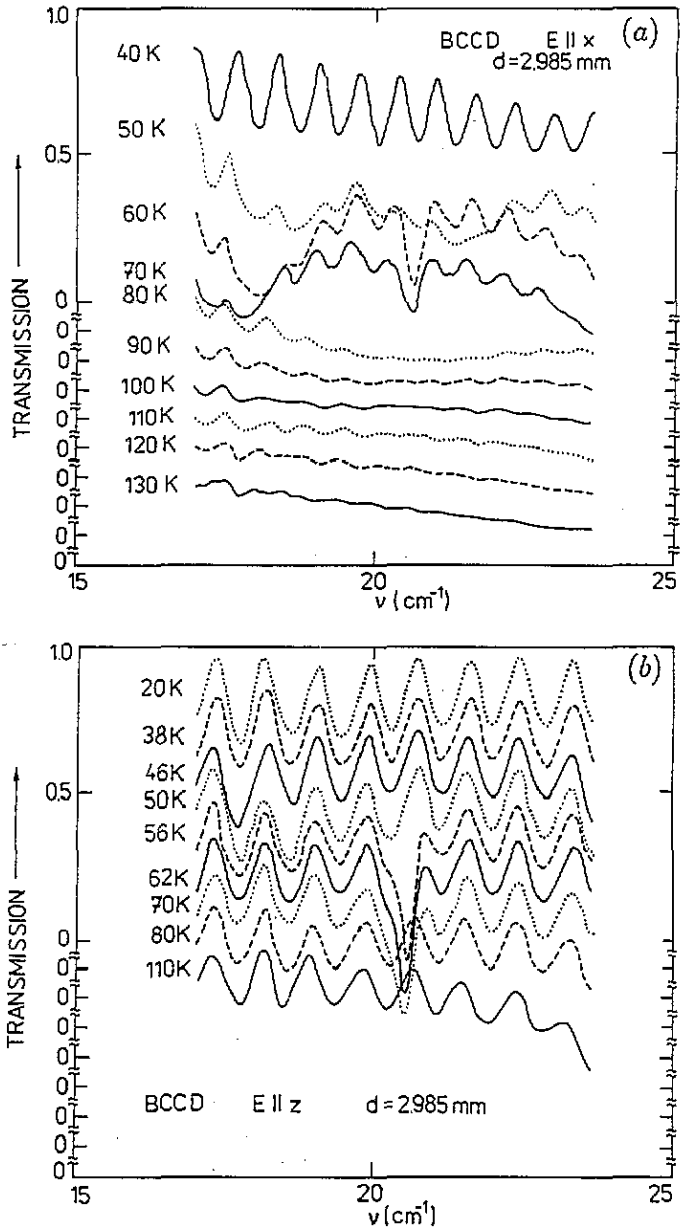

Figure 4. Temperature dependences of the submillimetre transmission spectra for (*a*) $E \| x$ and (*b*) $E \| z$ polarizations (thickness $d = 2.985$ mm).

All mode frequencies observed as a function of temperature are plotted in figure 6. For comparison we complemented our data by the earlier near-millimetre data (Volkov *et al* 1986, Goncharov *et al* 1988) and by the transmission data obtained by Ao and Schaack (1988a) and Ao (1990). Good agreement between all the data can be seen. In table 2 we list all observed mode frequencies for the high-temperature phase 1 and the low-temperature phase 17 up to about 300 cm^{-1}. At higher frequencies the quality of our polyethylene grid polarizer starts to deteriorate so that no unambiguous mode classification was possible.

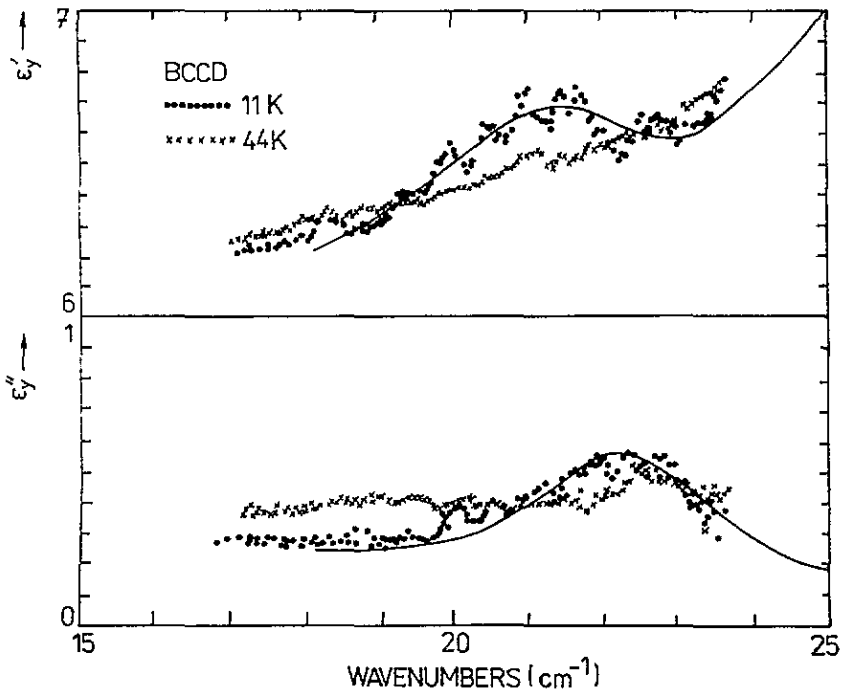

Figure 5. Complex dielectric spectrum $\epsilon_y = \epsilon_y' + \epsilon_y''$ in the submillimetre range at temperatures 44 and 11 K.

4. Discussion

4.1. Mode activity in non-modulated phases

First we consider the homogeneous (non-modulated) phases. Since the positions of atoms in the parent *Pnma* phase of BCCD are known (Brill *et al* 1985), it is easy to determine the symmetry of all 336 lattice vibrational modes at the Γ point (table 3). Obviously, we are interested mostly in low-frequency modes which should be looked for among 12 translational and 12 librational external modes. According to Dvořák (1990), the lowest-frequency librational modes are librations of betaines and Ca octahedra about axes in the x–z plane: an infrared-active mode $B_{2u}(y)$, a silent mode $A_u(xyz)$ and two Raman-active modes $B_{1g}(xy)$ and $B_{3g}(yz)$. It has been found experimentally that modes of just these symmetries have the lowest frequencies (at 270 K below 30 cm^{-1} (table 4)). We can obtain an idea of the lowest-frequency translational modes from the following simplified model of the BCCD structure; it is formed by two systems of layers parallel to (010) plane coupled by hydrogen bonds. Each layer consists of chains of BCCD molecules parallel to the x axis. Molecules within a chain are coupled by rather strong carboxyl bonds and therefore we shall consider chains as rigid units. The six degrees of freedom of two chains per unit cell are decomposed into three acoustic modes of B_{1u}, B_{2u} and B_{3u} symmetry and three translational optic modes of A_g, B_{1g} and B_{2g} symmetry. We believe that these optic modes are those modes in table 4 of frequencies less than 50 cm^{-1}. Inspecting again table 4 we observe that it remains to explain the origin of the B_{3u} mode (42 cm^{-1}). It could be one of the librational modes about the y axis which are of A_g, B_{1u}, B_{2g} and B_{3u} symmetry. The frequencies of librations about the y axis are expected to be higher than those of libraions

Table 2. Frequencies of observed IR modes below 300 cm^{-1} in the low- and high-temperature phases and their classification. The letters vw, w, m, s and vs in parentheses stand for very weak, weak, medium, strong and very strong IR strength, respectively. I stands for inhomogeneous ($q \neq 0$) modes; L stands for leakage from a different spectrum. Question marks stand for mode frequencies which cannot be evaluated but may be present in the spectra. The assignment is based on the assumption of orthorhombic symmetry of the ferroelectric phase.

$E \| x$			$E \| y$			$E \| z$		
Frequency (cm^{-1})			Frequency (cm^{-1})			Frequency (cm^{-1})		
15 K	170 K	Mode	15 K	170 K	Mode	15 K	170 K	Mode
32 (w)	—	B_{1g}	22 (vw)	—	A_u	31 (w)	(28)	B_{3g}
37 (w)	—	I	31 (vw)	—	A_u	37 (vw)	—	I
43 (w)	?	?	35 (vs)	15	B_{2u}	43 (vw)	—	$L(B_{3u})$
47 (vs)	44	B_{3u}	41 (s)	—	A_g	51 (w)	—	B_{3g}
52 (s)	—	B_{1g}	56 (m)	—	A_g	57 (vw)	—	I
57 (vw)	—	I	60 (w)	?	B_{2u}?	61 (m)	?	B_{1u}
64 (m)	—	B_{1g}	68 (w)	—	A_g	65 (m)	?	B_{1u}
68 (vw)	—	I	76 (m)	?	B_{2u}	74 (w)	—	B_{3g}
77 (m)	?	B_{3u}	87 (w)	—	A_u	88 (m)	86	B_{1u}
82 (w)	?	B_{3u}	104 (m)	—	A_g	93 (w)	—	B_{3g}
86 (w)	—	B_{1g}	109 (s)	107	B_{2u}	106 (vs)	104	B_{1u}
93 (s)	95	B_{3u}	113 (m)	?	B_{2u}	126 (m)	—	B_{3g}
105 (m)	—	B_{1g}	118 (m)	?	B_{2u}	140 (m)	138	B_{1u}
117 (s)	?	B_{3u}	167 (s)	164	B_{2u}	165 (w)	—	B_{3g}
126 (vs)	122	B_{3u}	184 (vs)	179	B_{2u}	179 (vs)	176	B_{1u}
133 (vs)	133	B_{3u}	205 (vs)	202	B_{2u}	203 (s)	?	B_{1u}
137 (vs)	?	B_{3u}	210 (m)	?	B_{2u}	211 (vs)	203	B_{1u}
157 (s)	149	B_{3u}	254 (m)	253	B_{2u}	223 (s)	222	B_{1u}
174 (m)	—	B_{1g}	303 (s)	298	B_{2u}	268 (s)	270	B_{1u}
213 (vs)	210	B_{3u}				292 (s)	294	B_{1u}
223 (s)	225	B_{3u}						
240 (s)	?	B_{3u}						
255 (m)	245	B_{3u}						
283 (s)	288	B_{3u}						

about axes in the x–z plane since they are connected with distortions of the carboxyl bonds between molecules.

It should be remembered that all modes discussed above should also be seen in various spectra of the proper ferroelectric phase depending on its point group symmetry. For convenience the corresponding selection rules are summarized in table 3. We present there also how the total number of modes and the total number of external modes in particular are distributed between symmetry species. Obviously, the number of translational optic and librational modes discussed previously is smaller than the total number of external modes since we have considered explicitly the lowest-frequency modes only.

In table 5 we list the compatibility between phonon modes along the Λ line of the Brillouin zone (BZ) ($q = \delta c^*$, $0 \leqslant \delta \leqslant \frac{1}{2}$) (Dvořák 1990) using the Λ notation used by Pérez-Mato (1988).

It is obvious that understanding the FIR spectra in the homogeneous proper ferroelectric phase 17 represents a clue for solving the question of the symmetry and number of order parameters frozen in this phase. Therefore we tried to compare all the available Raman data (Ao and Schaack 1988a, Ao 1990) and FIR data (Ao and Schaack 1988b, Ao 1990, Kamba *et al* 1990) (see also this work) to assign the low-frequency $q = 0$ modes. The

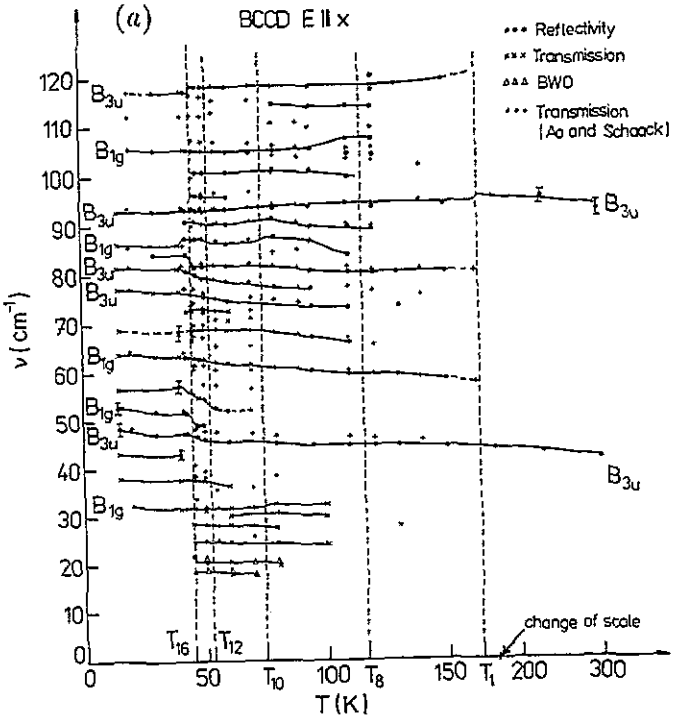
(a)
BCCD E ∥ x
••• Reflectivity
××× Transmission
ΔΔΔ BWD
••• Transmission (Ao and Schaack)
B3u
B1g
B3u
B1g
B3u
B3u
B1g
B1g
B3u
B1g
B3u
B3u
change of scale
T16
T12
T10
T8
T1
ν (cm⁻¹)
T (K)
0
50
100
150
200
300
10
20
30
40
50
60
70
80
90
100
110
120

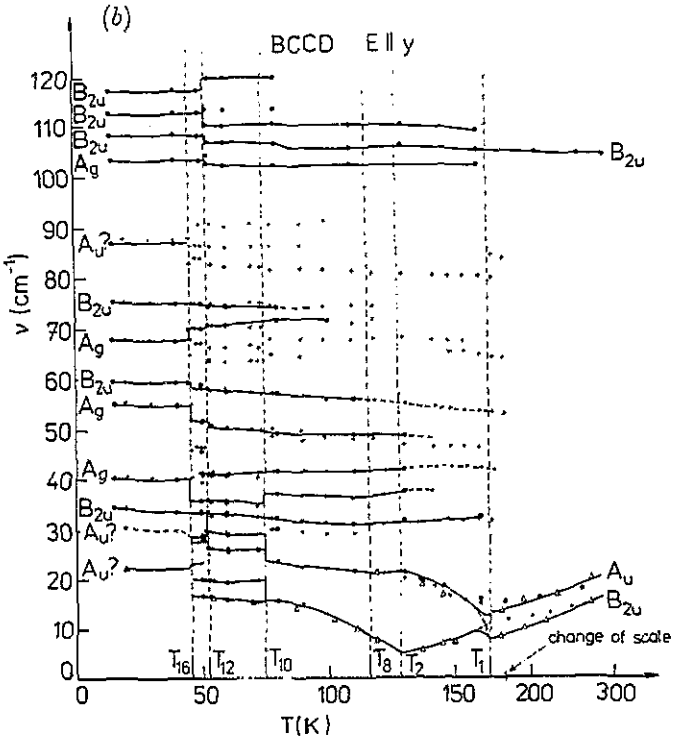
(b)
BCCD E ∥ y
B2u
B2u
B2u
Ag
B2u
Au?
B2u
Ag
B2u
Ag
Ag
B2u
Au?
Au?
Au
B2u
change of scale
T16
T12
T10
T8
T2
T1
ν (cm⁻¹)
T(K)
0
50
100
150
200
300
10
20
30
40
50
60
70
80
90
100
110
120

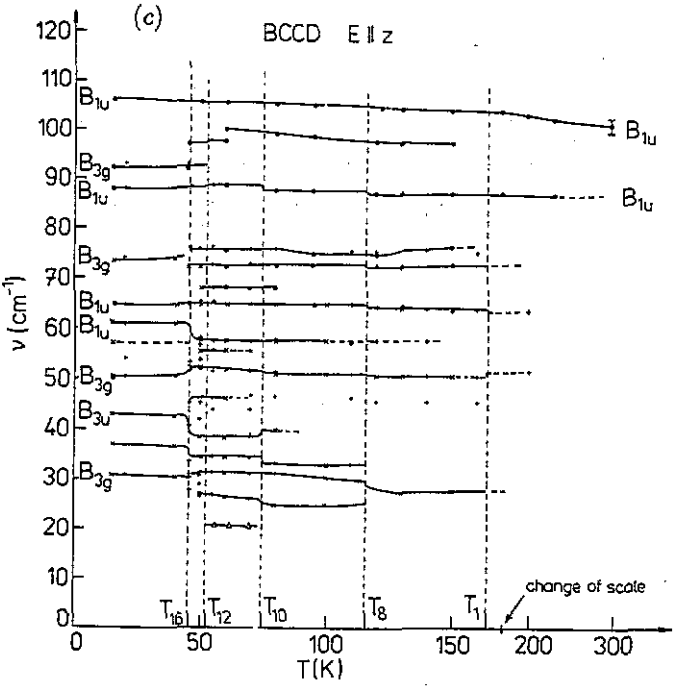

Figure 6. Temperature dependences of all the observed mode frequencies below 120 cm^{-1} for (*a*) $E \| x$, (*b*) $E \| y$ and (*c*) $E \| z$ polarizations. The results of different experiments (FIR reflectivity and transmission, BWO data from this work, and transmission data obtained by Ao (1990)) are denoted by different symbols.

Table 3. Factor-group analysis and mode activity of lattice vibrations in the parent and proper ferroelectric phases of BCCD. Both orthorhombic and monoclinic ferroelectric structures are considered. *ij*-type spectra ($i, j = x, y, z$) means activity in the Raman spectra with the non-zero α_{ij} Raman-tensor component; *i*-type spectra means IR activity for the $E \| i$ polarization.

	Number of Γ modes ($Z = 4$)							
			External BCCD			Symmetry species		
			Translational					
Type of spectrum	Total	Without hydrogen	Acoustic	Optic	Librational	*Pnma* (D_{2h}^{16})	$Pn2_1a$ (C_{2v}^{9})	$P12_11$ (C_2^2)
xx, yy, zz	46	23	—	2	1	A_g	A_1	A
y	38	16	1	—	2	B_{2u}	A_1	A
—	38	16	—	1	2	A_u	A_2	A
xz	46	23	—	2	1	B_{2g}	A_2	A
z	46	23	1	1	1	B_{1u}	B_1	B
yz	38	16	—	1	2	B_{3g}	B_1	B
xy	38	16	—	1	2	B_{1g}	B_2	B
x	46	23	1	1	1	B_{3u}	B_2	B

results for low-frequency modes up to 100 cm^{-1} are shown in table 4. Unfortunately, they are not quite unambiguous because the A_u modes are silent in the high-temperature phase and because some of the FIR transmission modes could not be seen at higher temperatures

Table 4. Zone-centre BCCD vibrations below 100 cm^{-1} in the high- and low-temperature phases. The type of spectrum in which the corresponding mode was observed is given in parentheses. In several cases (question marks) the IR mode frequencies could not be evaluated owing to the sample opacity and/or weakness in the reflectivity spectra. The high-temperature A_u modes are observed only in strained samples. The Raman data are taken from Ao (1990).

	Frequency (cm^{-1}) (spectrum type)				
D_{2h}	270 K	170 K	30 K	C_{2v}	Assignment
A_g	34 (xx, yy, zz)	36 (xx, yy, zz)	41 (yy, y)	A_1	T(x)
	48 (xx, yy, zz)	50 (xx, yy, zz)	56 (yy, y)		L(y)
	67 (zz)	68 (zz)	68 (yy, y)		
B_{2u}	16 (y)	9 (y)	34 (y, yy)	A_1	L(xz)
	?	53 (y)	60 (y, yy)		
	?	?	76 (y, xx)		
A_u	20 (y?)	15 (y?)	22 (y)	A_2	L(xz)
	?	32 (y?)	31 (xz, y)		
	?	?	87 (xz, y)		
B_{2g}	51 (xz)	51 (xz)	55 (xz, y?)	A_2	T(z)
	60 (xz)	58 (xz)	62 (xz, y?)		L(y)
	77 (xz)	74 (xz)	78 (xz, y?)		
B_{1u}	?	?	61 (z, yz)	B_1	L(y)
	?	64 (z)	65 (z, yz)		
	≃90 (z)	86 (z)	88 (z, yz?)		
B_{3g}	23 (yz)	21 (yz)	31 (yz, z)	B_1	L(xz)
	45 (yz)	46 (yz)	51 (yz, z)		
	70 (yz)	72 (yz)	74 (yz, z)		
	≃85 (yz)	≃88 (yz)	93 (yz, z)		
B_{1g}	27 (xy)	24 (xy)	32 (xy, x)	B_2	L(xz)
	46 (xy)	46 (xy)	52 (xy, x)		T(y)
	61 (xy)	60 (xy)	64 (xy, x)		
	77 (xy)	79 (xy)	86 (xy, x)		
	94 (xy)	96 (xy)	105 (xy, x)		
B_{3u}	?	?	43 (x, xy)	B_2	L(y)
	42 (x)	43 (x)	47 (x, xy)		
	?	?	77 (x, xy?)		
	?	?	82 (x)		
	?	95 (x)	93 (x, xy)		

owing to the sample opacity (see the question marks in table 4).

Table 4 now enables us to assign the FIR modes in table 2. However, we can see that there are several modes (e.g. the weak but sharp modes in the $E \| x$ and $E \| z$ spectra at 37 and 57 cm^{-1}) which cannot be assigned to any of the Γ-point modes from table 4. It seems that our sample was not quite homogeneous at low temperatures, containing still some admixture of modulated phases. In analogy to a stressed sample (Brill and Ehses 1985) it would seem natural that the modulated part has $\delta = \frac{1}{6}$, but our data are not conclusive. The conclusion about the coexistence of two phases in the ferroelectric region and also in some intermediate phases comes from several other recent experiments (Almeida *et al* 1992,

Table 5. Compatibility relations along the Λ line.

$q = 0$ Γ point	$q = \delta c^*$ Λ line	$q = \frac{1}{2}c^*$ Z point
B_{2u} (y)	$P(k)$ (Λ_3)	Z_2
B_{3g} (yz)	$P(k)$ (Λ_3)	Z_2
A_u (xyz)	$Q(k)$ (Λ_2)	Z_2
B_{1g} (xy)	$Q(k)$ (Λ_2)	Z_2
B_{2g} (xz)	$p(k)$ (Λ_4)	Z_1
B_{3u} (x)	$p(k)$ (Λ_4)	Z_1
A_g (xx, yy, zz)	$q(k)$ (Λ_1)	Z_1
B_{1u} (z)	$q(k)$ (Λ_1)	Z_1

Zúñiga *et al* 1991). The macroscopic inhomogeneity of the ferroelectric phase makes the assignment of all FIR modes and therefore the decision about the actual symmetry of this phase extremely difficult.

Nevertheless, in tables 2 and 4 our classification is mostly consistent with the orthorhombic symmetry, except for a few weak inhomogeneous modes or one leakage mode. The most serious complication is the activity of the theoretically silent A_u mode near 20 cm^{-1} (Goncharov *et al* 1988). In the clamped sample this mode is IR active in all phases, but in the low-temperature ferroelectric phase 17 its strength drops jumpwise. The assumption that this mode is an A_u mode is supported by inelastic neutron scattering results (Currat *et al* 1990) which in combination with symmetry arguments require the existence of an A_u mode near 20 cm^{-1}. However, in the stress-free sample this mode is not seen in phase 1 and it is only extremely weakly activated in the low-temperature phase 17 (see figure 5). Our attempts to influence its IR strength in phase 1 by external σ_{xz} stress inducing monoclinic symmetry gave no unambiguous results. In the low-temperature phase 17 also the other A_u modes remain weakly IR active as can be deduced from the xz Raman activation of the same modes in this phase. This would mean that some monoclinic distortions are present in the low-temperature phase and that the A_u modes are extremely sensitive to them. However, no other clear features derived from table 3 that would support monoclinicity can be seen. Another possibility would be that the weak A_u modes are in fact inhomogeneous modes from the same optical branches as the A_u modes due to a small admixture of the modulated phase $\frac{1}{5}$ (see figure 7(d)).

4.2. Mode activity in the modulated phases

As a consequence of the C or IC modulation of the parent phase, many modes originally inside the BZ of the parent lattice may become Raman and/or IR active. In general, owing to the change in crystal structure, some modes originally inactive (in particular, modes with wavevector $q \neq 0$) acquire symmetries of active Γ-point modes. Hence, bilinear coupling between these modes and active Γ-point modes becomes possible in a modulated phase with coupling constants proportional to some power of the frozen soft-mode amplitude η. Such a bilinear coupling is in fact induced by the frozen soft mode in a modulated phase via anharmonic interaction terms in the parent phase between the soft mode, an active Γ-point mode and a particular activated mode (Petzelt and Dvořák 1976). Allowed anharmonic terms can be easily found using group theory and in this way we can determine the new active modes in modulated phases. (Independently the problem of new Raman-active modes in modulated phases has been recently studied by Poulet and Pick (1992) with essentially the same results.) Although complete general results for IC as well as for all possible C phases are available, we shall list only those activated modes which are of practical interest. As

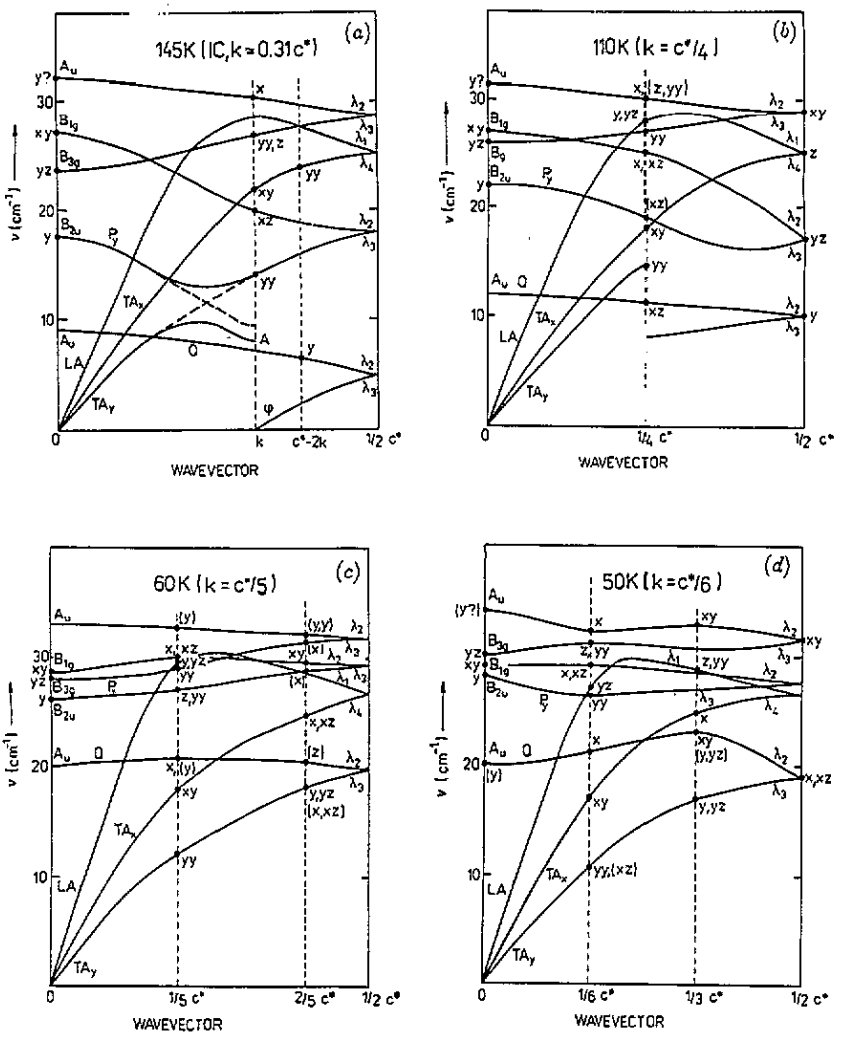

Figure 7. Semiquantitative suggestion for the eight lowest phonon dispersion branches of the main phases at temperatures of (*a*) 145 K (IC), (*b*) 110 K ($\delta = \frac{1}{4}$), (*c*) 60 K ($\delta = \frac{1}{5}$) and (*d*) 50 K ($\delta = \frac{1}{6}$). The modes observed for various IR (x, y, z) and Raman (yy, xy, xz, yz) spectra are denoted. The symbols of spectra in parentheses denote activation due to higher-order processes (third order in figure 4(*b*), third and fourth order in figure 4(*c*) and fourth, fifth and sixth order in figure 4(*d*)). All the minigaps except the amplitudon–phason splitting are neglected.

discussed above, the activation of modes is a morphic effect, i.e. the strengths of activated modes in various spectra are proportional to some power of η. Obviously, if such a power is too high, the new modes could be hardly detected in the spectra, at least not far below T_1.

In general, if a soft mode of wavevector k is frozen in the structure, modes at $\mp nk$ ($n = 1, 2, 3, \ldots$) may become active. Since the degeneracy of modes at nk and $-nk$ is lifted by their interaction induced by the frozen soft mode (Dvořák 1980), each of the activated modes is in fact a doublet. We expect this splitting not to be resolved owing to the finite linewidth, except possibly for modes at $\mp k$.

Let us discuss first the IC phase. Modes at $\mp k$ are activated by cubic normal coupling

terms (the sum of wavevectors of coupled modes is zero) and their strength is proportional to η^2. As a rule, one component of the doublet is Raman active and the other is IR active. Since, in the IC phase of BCCD, $k > \frac{1}{4}c^*$, modes at $\mp 2k$ are activated by quartic umklapp terms; their strength is proportional to η^4. It can be shown that modes activated at higher multiples of k have strengths proportional to powers of η higher than four. The results of our analysis are summarized in table 6. It should be stressed that, since the results for an IC phase are valid for an arbitrary value of k, they are valid for C values of k too, i.e. for all C phases. Special attention is required to analyse the light scattering activity of the $q \to k$ (nearly uniform) phason. Using the approach of Poulet and Pick (1981), the phason with the small wavevector along the a, b and c axes should be active in the xz, yz and ii ($i = x, y, z$) spectra, respectively.

Table 6. Activity of the phonon branches in different spectra in modulated phases with an arbitrary wavevector k (smaller than $\frac{1}{3}c^*$) induced by the frozen soft-mode amplitude $P_k(\Lambda_3) \equiv \eta$. The strength of modes at the frozen-in wavevector k is proportional to η^2 and those at $2k$ and $3k$ to η^4 and η^6, respectively. Actually the activity rules are the same for all modes with even ($2nk$) and odd ($(2n+1)k$) multiples of k, respectively; the strengths of modes are proportional to η^{4n} and η^{4n+2}, respectively.

	Active wavevectors				
Spectrum	k	$2k \leqslant \frac{1}{2}c^*$	$c-2k \leqslant \frac{1}{2}c^*$	$3k \leqslant \frac{1}{2}c^*$	$c^*-3k \leqslant \frac{1}{2}c^*$
xx, yy, zz	Λ_3	Λ_1	Λ_4	Λ_3	Λ_2
z	Λ_3	Λ_1	Λ_4	Λ_3	Λ_2
—	Λ_4	Λ_2	Λ_3	Λ_4	Λ_1
xy	Λ_4	Λ_2	Λ_3	Λ_4	Λ_1
yz	Λ_1	Λ_3	Λ_2	Λ_1	Λ_4
y	Λ_1	Λ_3	Λ_2	Λ_1	Λ_4
xz	Λ_2	Λ_4	Λ_1	Λ_2	Λ_3
x	Λ_2	Λ_4	Λ_1	Λ_2	Λ_3

In C phases, new unklapp anharmonic terms become effective in activating new modes in various spectra depending on the particular symmetry of the C phase. However, it turns out (see Poulet and Pick (1992) for a detailed discussion), that none of these new active modes specific of a C phase could have a sufficient strength for producing specific features in Raman and/or IR spectra of C phases.

Strictly speaking, one effect of commensurability could be eventually detected provided that the symmetry of the C phase is the lowest possible, i.e. $P1c1$ for $k = (m^-/n^+)c^*$, $P112_1$ for $k = (m^-/n^-)c^*$, $Pn11$ for $k = (m^+/n^-)c^*$ where $+$ and $-$ denote even and odd integers, respectively. In these cases both components of doublets at $\mp k$ would be active simultaneously in the same spectra.

On the basis of the selection rules discussed above (see table 6) and our IR and published Raman data (Ao and Schaack 1988a, b, Wilhelm and Unruh 1991) we suggest semiquantitatively the shape of eight lowest phonon dispersion branches in the main phases at temperatures of 145, 110, 60 and 50 K (figure 7). We did not attempt to construct dispersion branches at higher frequencies (above 30 cm^{-1}) because of the incomplete published Raman data and the large number of branches which make the assignment ambiguous. To explain all observed IR and Raman modes we had to use frequently the

activation of phonons at $2k$ or $3k$. One can see a tendency towards activation by higher-order effects upon decreasing temperature (increasing the magnitude of the spontaneous order parameter). In the modulated phase 13 with $\delta = \frac{1}{6}$, activation up to $5k$ was needed to explain the very weak xz Raman mode and up to $6k$ to activate the Γ-point A_u mode in the $E \| y$ spectra.

Considering also higher-order activation processes we succeeded in explaining all modes assuming a single order parameter. Now, we shall make some comments on some of our mode assignments. The first comment concerns the ferroelectric soft mode which according to Volkov *et al* (1986) seemed to soften further below T_1 down to about $T_2 \simeq 128$ K. Such behaviour has not been understood so far. Our reflectivity data together with the transmission data obtained by Ao (1990) show, however, clearly that this mode starts to harden already at T_1, which could be naturally expected if for example the whole soft optic Λ_3 branch hardened below T_1 (see figures 7(a) and 7(b)). On lowering the temperature, this mode—which is by far the strongest low-frequency mode in the $E \| y$ spectra—continues to harden up to about 34 cm^{-1} anti-crossing at least two weaker modes near 30 cm^{-1} (see figure 6(b)).

Below T_1, the lowest-frequency allowed mode in the $E \| y$ spectra becomes the $\Lambda_2(c^* - 2k)$ mode (see figure 7(a)). It further softens in the IC phase because it increases its wavevector upon decreasing temperature and shifts in this way along the Λ_2 branch with negative dispersion. Below T_2, some hardening of this branch could be expected as a commensurability gap should develop in the phason spectrum. Below T_3 the $\Lambda_2(c^* - 2k)$ mode further shifts towards the BZ boundary but owing to slight hardening of the phason branch no pronounced temperature dependence of its frequency is observed. Finally, at T_8 ($\delta = \frac{1}{4}$) the $\Lambda_2(c^* - 2k)$ mode is locked at the BZ boundary and the whole branch starts to harden progressively owing to the growth of the pseudophason gap at $k = \frac{1}{4}c^*$. This shows up by the hardening of the $\Lambda_2(\frac{1}{2}c^*)$ mode in the $E \| y$ spectra within the C phase 9 (see figure 6(b)). At $T_{10} = 75$ K the lowest-frequency y-active mode becomes the $\Lambda_3(\frac{2}{5}c^*)$ mode on the lowest TA_y acoustic branch. The second new mode in the y spectrum at about 20 cm^{-1} (see figure 6(b)) could be the $\Lambda_2(\frac{1}{5}c^*)$ mode activated by a fourth-order process. At $T_{12} = 53$ K the former mode changes to $\Lambda_2(\frac{1}{3}c^*)$ and the Γ-point A_u mode may become active owing to the sixth-order process provided that the phase 13 is monoclinic (see below). Such a high-order process could be operative because the activation is resonantly enhanced by the close vicinity of the strong ferroelectric $P_y(0)$ mode. Finally below $T_{16} = 46$ K the strengths of these modes drop almost to zero. The origin of the extremely weak mode at 22 cm^{-1} (see figure 5) is not clear and suggests a weak monoclinicity and/or inhomogeneity of our sample.

As we have already pointed out, the A_u modes can be seen in the $E \| y$ spectra of phases 13–17 only if these phases are monoclinic. Such a symmetry can be achieved by an appropriate choice of the phase φ of the order parameter P_y (Pérez-Mato 1988) in the phases 13, 14, 15 and 16. Unfortunately there are two difficulties with the phases 13, 14 and 16: the phase φ should have a general value which is rather unlikely and the spontaneous P_z component should exist which, however, has not been detected so far. As for the proper ferroelectric phase 17 it can never be monoclinic (2_y) unless two modes of different symmetries (Λ_2 and Λ_3) are frozen simultaneously. Actually this was one of the reasons why the concept of two order parameters was introduced for BCCD (Dvořák *et al* 1988).

A further comment concerns the amplitudon A (see figure 7(a)) which appears on the acoustic Λ_3 branch hydridized with the optic $P_y(q)$ branch of the same symmetry. Wilhelm and Unruh (1991) in their yy Raman spectra apparently have seen the higher mode on the

$P_y(q)$ branch which did not soften sufficiently on approaching T_1 from below as it was coupled to a lower-lying overdamped mode. We propose that the latter mode is the proper amplitudon (see figure 7(*a*)) which should be also active in the $E \| z$ spectra (see table 6). Also the pseudophason should become active in z spectra. Unfortunately, our present IR data are limited to $\nu > 17$ cm^{-1} (see figure 4(*b*)) so that no direct conclusion concerning the amplitudon and pseudophason behaviours is possible. Indirect conclusions are available from the behaviour of the lowest-frequency y and xz modes. On lowering the temperature, it seems that the phason gap rapidly increases (especially in the $\delta = \frac{1}{4}$ phase 9) and the amplitudon–pseudophason splitting decreases owing to the hardening of the whole phason branch Λ_3 and its Λ_2 continuation (figures 6(*b*) and 7(*b*)).

We note that our assignment differs from that in our previous papers (Kamba *et al* 1990, Dvořák 1990) where only the lowest second-order activation processes have been considered. The basic change concerns, however, the assignment of the two lowest optic branches below T_1. Previously we have assigned the lowest $E \| y$ mode to the $q = 0$ mode on the P_y branch and the next y mode to the $q = 0$ (A_u) mode on the Q branch. Now we believe that the actual sequence of branches is reversed. In the previous papers we came to the conclusion that the modulated phases have monoclinic symmetry which (at least in the case of the IC structure) implies two frozen order parameters. Since that time all the experiments (Wilhelm and Unruh 1991, Zúñiga *et al* 1991, Ezpeleta *et al* 1992) seem to support the single-order-parameter picture and the orthorhombic symmetry in all phases (at least above 80 K). Our results support this single-order-parameter picture and the orthorhombic symmetry down to about $T_{12} = 53$ K. At lower temperatures there are some indications of sample monoclinicity and/or inhomogeneity from our data. The mode assignment still suffers from some ambiguity at these temperatures.

5. Conclusions

Symmetry and wavevector classification of all modes observed in our FIR spectroscopy study of BCCD was attempted, using the group-theoretical analysis of the selection rules of IR and Raman vibrational mode activity in all phases and analysing also the available Raman data. It was possible to explain almost all the new activated modes in the phases with $\delta =$ IC, $\frac{1}{4}$, $\frac{1}{5}$, $\frac{1}{6}$, 0 by the freezing of a single order parameter of Λ_3 symmetry ($P_y(k)$ wave). On lowering the temperature, higher-order processes become operative in activating the modes. In the $\delta = 0$ low-temperature phase some traces of weak monoclinicity and/or modulated phases are seen which might also be caused by local stresses.

On the basis of our mode assignment we attempted to construct semiquantitatively the dispersion curves of the eight lowest phonon branches along the modulation direction c^* for the four main modulated phases ($\delta =$ IC, $\frac{1}{4}$, $\frac{1}{5}$, $\frac{1}{6}$). From the discussion of the phason and amplitudon behaviour it becomes apparent that in the IC phases both excitations should be overdamped and lie below 10 cm^{-1}. In the C phase 9 ($\delta = \frac{1}{4}$) the gap in the pseudophason spectrum rapidly increases and the amplitudon–pseudophason splitting decreases, but no quantitative conclusions can be drawn. More accurate investigations of the IR $E \| z$ and xz Raman spectra below about 15 cm^{-1} are needed, especially in the $\delta = \frac{1}{4}$ phase (115–75 K). Also the question of the low-temperature behaviour of the A_u modes in the $E \| y$ spectra needs more thorough investigation. New measurements on fully deuterated samples are in progress.

Acknowledgments

We would like to thank J Albers and A Klöpperpieper for providing the crystals, R Pick for many fruitful discussions and the preprint of the paper by Poulet and Pick (1992) and G Schaack for providing the dissertation by Ao.

References

Almeida A, Chaves M R, Kiat J M, Schneck J, Schwarz W, Tolédano J C, Ribeiro J L, Klöpperpieper A, Müser H E and Albers J 1992 *Phys. Rev.* B **45** 9576
Ao R 1990 *Dissertation* University of Würzburg
Ao R and Schaack G 1988a *Ferroelectrics* **80** 105
—— 1988b *Indian J. Pure Appl. Phys.* **26** 124
Ao R, Schaack G, Schmidt M and Zöller M 1989 *Phys. Rev. Lett.* **62** 183
Brill W and Ehses K 1986 *Japan. J. Appl. Phys.* **24** 826
Brill W, Schildkamp W and Spilker J 1985 *Z. Kristallogr.* **172** 281
Currat R, Legrand J F, Kamba S, Petzelt J, Dvořák V and Alberts J 1990 *Solid State Commun.* **75** 345
Dvořák V 1980 *Lecture Notes in Physics* vol 115 (Berlin: Springer) p 447
—— 1990 *Ferroelectrics* **104** 135
—— 1991 *Phase Trans.* **31** 23
Dvořák V, Holakovsky J and Petzelt J 1988 *Ferroelectrics* **79** 15
Dvořák V, Janovec V and Ishibashi Y 1983 *J. Phys. Soc. Japan* **52** 2053
Ezpeleta J M, Zúñiga F J, Perez-Mato J M, Paciorek W A and Breczewski T 1992 *Acta Crystallogr.* B **48** 261
Freitag O and Unruh H G 1990 *Ferroelectrics* **105** 357
Goncharov Yu G, Kozlov G V, Volkov A A, Albers J and Petzelt J 1988 *Ferroelectrics* **80** 221
Haussühl S, Liedtke J, Albers J and Klöpperpieper A 1988 *Z. Phys.* B **70** 219
Kamba S, Petzelt J, Dvořák V, Goncharov Yu G, Volkov A A, Kozlov G V and Albers J 1990 *Ferroelectrics* **105** 351
Kobayashi J and Kleeman W 1990 *Ferroelectrics* **105** 213
Kroupa J, Albers J and Ivanov N R 1990 *Ferroelectrics* **105** 345
Pérez-Mato J M 1988 *Solid State Commun.* **67** 1145
Petzelt J and Dvořák V 1976 *J. Phys. C: Solid State Phys.* **9** 1571
Poulet H and Pick R M 1981 *J. Phys. C: Solid State Phys.* **14** 2675
—— 1992 *J. Birman's Festschrift* ed M Balkanski, M Lax and H R Trebin (Singapore: World Scientific)
Ribeiro J L, Chaves M R, Almeida A, Muser H J, Albers J and Klöpperpieper A 1990 *Ferroelectrics* **105** 363
Rother H J, Albers J and Klöpperpieper A 1984 *Ferroelectrics* **54** 107
Unruh H G, Hero F and Dvořák V 1989 *Solid State Commun.* **70** 403
Uesu Y and Kobayashi J 1985 *Ferroelectrics* **64** 115
Volkov A A, Goncharov Yu G, Kozlov G V, Albers J and Petzelt J 1986 *Pis. Zh. Eksp. Teor. Fiz.* **44** 469
Volkov A A, Goncharov Yu G, Kozlov G V, Lebedev S P and Prokhorov A M 1985 *Infrared Phys.* **25** 369
Wilhelm H and Unruh H G 1991 *Z. Kristallogr.* **195** 75
Zúñiga F J, Ezpelela J M, Pérez-Mato J M, Paciorek W A and Madariaga G 1991 *Phase Transitions* **31** 29